Bioorganic & Medicinal Chemistry 17 (2009) 653–659

Contents lists available at ScienceDirect

Bioorganic & Medicinal Chemistry

journal homepage: www.elsevier.com/locate/bmc

Development of an optimized activatable MMP-14 targeted SPECT imaging probe

Gregory A. Watkins [a], Ella Fung Jones [a,*], M. Scott Shell [b], Henry F. VanBrocklin [a,c], Mei-Hsiu Pan [a], Stephen M. Hanrahan [c], Jin Jin Feng [a], Jiang He [a], Nor Eddine Sounni [d], Ken A. Dill [b], Christopher H. Contag [e], Lisa M. Coussens [d], Benjamin L. Franc [a]

[a] Center for Molecular and Functional Imaging, Department of Radiology and Biomedical Imaging, University of California, San Francisco, 185 Berry Street, Suite 350, Box 0946, San Francisco, CA 94107, United States
[b] Department of Pharmaceutical Chemistry, University of California, San Francisco, San Francisco, CA 94143, United States
[c] Department of Functional Imaging, Lawrence Berkeley National Laboratory, Berkeley, CA 94720, United States
[d] Department of Pathology, University of California, San Francisco, San Francisco, CA 94115, United States
[e] Departments of Pediatrics, Radiology, and Microbiology & Immunology, Molecular Imaging Program Stanford University, Stanford, CA 94305, United States

ARTICLE INFO

Article history:
Received 7 October 2008
Revised 18 November 2008
Accepted 23 November 2008
Available online 6 December 2008

Keywords:
Cancer
MMP-14
Protease sensitive probe
SPECT imaging

ABSTRACT

Matrix metalloproteinase-14 (MT1-MMP or MMP-14) is a membrane-associated protease implicated in a variety of tissue remodeling processes and a molecular hallmark of select metastatic cancers. The ability to detect MMP-14 in vivo would be useful in studying its role in pathologic processes and may potentially serve as a guide for the development of targeted molecular therapies. Four MMP-14 specific probes containing a positively charged cell penetrating peptide (CPP) d-arginine octamer (r_8) linked with a MMP-14 peptide substrate and attenuating sequences with glutamate (8e, 4e) or glutamate-glycine (4eg and 4egg) repeating units were modeled using an AMBER force field method. The probe with 4egg attenuating sequence exhibited the highest CPP/attenuator interaction, predicting minimized cellular uptake until cleaved. The in vitro MMP-14-mediated cleavage studies using the human recombinant MMP-14 catalytic domain revealed an enhanced cleavage rate that directly correlated with the linearity of the embedded peptide substrate sequence. Successful cleavage and uptake of a technetium-99m labeled version of the optimal probe was demonstrated in MMP-14 transfected human breast cancer cells. Two-fold reduction of cellular uptake was found in the presence of a broad spectrum MMP inhibitor. The combination of computational chemistry, parallel synthesis and biochemical screening, therefore, shows promise as a set of tools for developing new radiolabeled probes that are sensitive to protease activity.

Published by Elsevier Ltd.

1. Introduction

Tumor cells employ a host of biochemical mechanisms in order to invade and metastasize. Many of these mechanisms are thought, in part, to involve proteases associated with cell membrane and extracellular matrix (ECM) molecules that are posited to initiate pro-angiogenic signaling cascades. Among cancer-associated proteases, matrix metalloproteases (MMPs), a class of zinc-dependent proteolytic enzymes, have been postulated to be used by cancer cells to dissolve ECM during neoplastic progression.[1] In addition, numerous studies have documented a positive correlation between certain MMP expression levels and poor outcome in cancer patients.[2] The importance of MMPs in tumor progression not only has guided the development of MMP inhibitors for therapy, it has also received particular attention as imaging target utilizing methods to detect tumor-associated proteolytic activity in vivo.[3–7]

The family of human MMPs contains 16 secreted and 7 membrane-tethered enzymes.[8] A subclass of the membrane-anchored proteinases, termed membrane type (MT) MMPs, plays dominant roles in controlling cancer cell behavior.[9,10] In particular, the up-regulation of the membrane-associated collagenase MMP-14 (MT1-MMP) correlates to the invasiveness of many different tumor types.[2] MMP-14 not only promotes tumor growth through induction of angiogenesis and proteolysis of ECM, but it also acts as a critical regulatory switch in the activation of MMP-2 proenzyme.[11] Clinical studies revealed that the expression of MMP-14 is associated with poor prognosis in patients with advanced neuroblastoma,[12] small cell lung cancer (SCLC),[13] tongue squamous cell carcinoma,[14] head and neck carcinoma,[15] bladder, and ovarian cancer.[16,17] MMP-14 has been detected in tumor cells and

* Corresponding author. Tel.: +1 415 353 9469; fax: +1 415 353 9423.
E-mail address: ella.jones@radiology.ucsf.edu (E.F. Jones).

0968-0896/$ - see front matter Published by Elsevier Ltd.
doi:10.1016/j.bmc.2008.11.078

adjacent stromal cells in a variety of human tumors including breast.[9] Consequently, MMP-14 overexpression holds great promise as an early biomarker for invasive cancers.

In the past, several in vivo optical imaging probes targeting various MMPs have been reported; the most successful of these efforts have been directed against MMP-2, -7, and -9.[18–23] Attempts to image MMP activities by non-optical modalities (e.g., positron emission tomography (PET) or single photon emission computed tomography (SPECT)) using labeled substrates or inhibitors, however, have met with limited success in vivo, in part due to the poor specificity and in vivo stability of the radiolabeled probes.[24–31] Our motivation, therefore, was to develop a sensitive nuclear probe for MMP-14 activities for early cancer detection. The success of such a probe would represent a significant advancement in preclinical and clinical imaging as it would be a tool able to locate and track the molecular evolution of malignant tissues for use in drug development.

A number of protease imaging strategies have been described previously. One particular class of probes comprising an 'activatable' delivery mechanism has been developed by a number of research groups.[21,23,32] These probes share a core structure consisting of a poly-D-arginine cell penetrating peptide (CPP) that is covalently tethered to a negatively charged attenuating peptide sequence through a proteolysis sensitive peptide (Fig. 1). The intact probe is believed to be prohibited from crossing the cell membrane due to the electrostatic interaction between the positively charged arginine and the tethered intramolecular negatively charged attenuator (I), but other mechanisms may also contribute. However, proteolytic cleavage (II) separates the polyarginine sequence from the negatively charged domain, thereby triggering uptake of the CPP (III). Protease-rich tissues may be imaged by tagging an imaging reporter group, such as a fluorophore, gadolinium chelate or radionuclide, to the CPP.[32] As a result, the number of protease cleavage events may be correlated to the CPP concentration, and its associated tag, within targeted cells. Using agents directed against MMP-2/9 and -7, Rao and co-workers have selectively tagged cultured fibrosarcoma cells (HT-1080) with quantum dots,[23] while Tsien and co-workers successfully imaged cancers rich in MMP-2 and -9 in murine xenografts, using optical and magnetic resonance techniques.[21]

This general strategy is attractive because the catalytic processing of more than one probe by each enzyme provides a robust mechanism for signal amplification. For the purpose of MMP-14 imaging, this is a particularly important point if one seeks to detect protease activity prior to the maturation of secondary downstream proteases, for example, MMP-2 and -9.

The development of an 'activatable' SPECT imaging probe specific for MMP-14 is reported herein. The probe design was undertaken realizing that attaching a large metal chelate for nuclear imaging may alter the topology of the MMP-14 selective peptide sequence and adversely affect the cleavage rate as well as attenuation characteristics of the basic probe platform. Therefore the combination of molecular modeling, parallel synthesis and bioassay screens were effectively utilized to optimize the imaging probe construct for MMP-14 activities. This work sheds new light on the intramolecular quenching and activation mechanisms of this class of imaging peptides, and demonstrates the value of computational chemistry relative to imaging probe development.

2. Results and discussion

2.1. MMP-14 probe design and modular components

The general MMP-14 probe, shown in Figure 2, is a modular design comprised of three components: (A) a positively charged d-arginine octamer (r_8) cell penetrating peptide (CPP) attached with single amino acid chelate (SAAC) for technetium-99m; (B) a MMP-14 specific cleavable substrate (SGRIGF↓LRTA) and (C) a negatively charged attenuation sequence. The seminal component for designing an effective MMP-14 probe was a suitable cleavable peptide substrate. A known MMP-14 substrate (SGRIGF↓LRTA) was incorporated into our constructs to maximize the selectivity of the probe for MMP-14-rich tissues. This sequence was originally described by Smith and co-workers, who employed phage display technology to map the substrate specificity of matrix metalloproteinases.[33] In an enzyme panel study, this peptide sequence is preferentially cleaved by MMP-14 with a k_{cat}/K_m value of 777,200 M^{-1}/s, while the cleavage by the related MMP-9 is much less efficient, with a k_{cat}/K_m of 20,000 M^{-1}/s.

Although poly-D-arginine sequences with chain lengths of 7–14 residues have been widely employed as cell membrane penetrating transporters[34] in probe constructs, there has been little consensus over the degree of attenuation necessary for effective proteolytic cleavage and reducing cell penetration. In designing the MMP-14 probe, the attenuation module was optimized considering: (1) the number of negatively charged residues for effective attenuation; (2) the structural impact on the cleavable peptide sequence

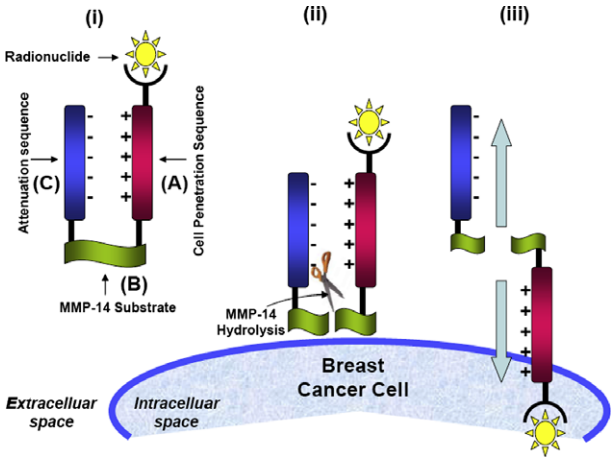

Figure 1. Outline of the probe structure and mechanism. The quenched probe (I) is able to freely circulate in vivo, until it encounters its protease target. Cleavage of the probe at a defined point by MMP-14 (II) releases a cell penetrating peptide, which can then translocate its radionuclide cargo across the target cell membrane (III). After uncleaved quenched probe is washed away, the internalized radioactivity can be imaged by SPECT.

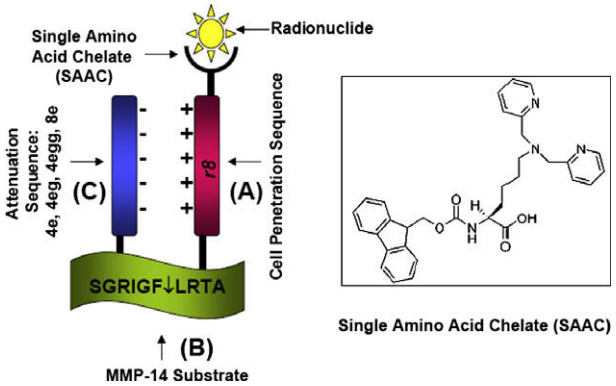

Figure 2. The general modular design of the MMP-14 probe comprising: (A) positively charged arginine octamer (r8) cell penetrating peptide with the single amino acid chelate (SAAC) coordinated with a radionuclide; (B) MMP-14 peptide substrate (SGRIGF↓LRTA) and (C) variation of D-glutamate attenuation sequences (4e, 4eg 4egg and 8e).

and (3) the ability to release the cleaved probe for cellular uptake. Attenuation of D-arginine octamer (r_8) CPP was favorably achieved by inserting the optimal number of D-glutamate residues in the attenuation domain, such that the cleavable peptide sequence was present in a roughly linear conformation and available for docking to the MMP-14 enzyme. A small panel of attenuation sequences, including four D-glutamates (4e), four D-glutamate-glycine repeats (4eg), four D-glutamate-glycine-glycine repeats (4egg) and eight contiguous D-glutamates (8e), were evaluated using computer modeling. The D version of the amino acid residues were chosen to prevent non-specific in vivo proteolysis. Based on prior experience, the choice of four D-glutamates appropriately spaced in three of the four attenuator sequences adequately attenuates the r_8 peptide.[32]

Finally, in order to conduct radionuclide imaging by SPECT, it is necessary to selectively label the peptide probe with a suitable isotope. To this end, the single amino acid chelate (SAAC) technology, previously developed by Stephenson et al.,[35,36] has been utilized. The SAAC is a Nε-bis(pyridylmethyl)-lysine derivative that may be site-selectively incorporated into synthetic peptides using standard Fmoc chemistry. The resulting compounds carry an N-3 chelator that form stable tricarbonyl complexes with technetium and rhenium. Technetium-99m, a gamma ray emitter, has emissions of sufficient energy (140 keV) to penetrate the human body, but not too energetic to pass through the SPECT detector material. It is considered to be a near-ideal isotope for SPECT imaging, in part due to its short half-life (6 h), its gamma emission energy and its availability from a commercial generator system. Based on these characteristics, technetium-99m has been chosen in the current probe design to visualize cell penetration upon proteolysis.

2.2. Computational chemistry

Holding the CPP and MMP-14 peptide regions constant and using the cysteine–cysteine disulfide bond as a linker between modules, the overall structure with four different attenuation sequences containing D-glutamate residues (4e, 4eg , 4egg and 8e) was computed. The extent of charge-complementation was calculated between the CPP and the attenuation sequence by examining the number of arginine residues that were in contact with the glutamate residues. The average end-to-end backbone length of the cleaved substrate was measured to quantify the extent of exposed substrate, in an available extended conformation, for effective enzyme pocket binding for subsequent cleavage by the MMP-14. Based on these calculations, the dominant conformation for each probe, shown in Figure 3, was determined.

These dominant structures reveal that the 4e probe has minimum interaction between the CPP (blue) and the attenuation sequence (red). Structural calculations confirm the overlap finding (Fig. 4A) with the 4e probe possessing the least CPP-attenuator complementation at an average of 4.3 ± 1.5 arginine residues in contact with D-glutamate while contact in the other three probes range from 5.2 ± 1.6 to 6.4 ± 1.2 residues. Here, the standard deviation reported does not indicate the standard error in the measurement. Instead, it corresponds to the root mean square fluctuation of the measurement within the computed peptide conformational ensemble, that is due to the natural conformational fluctuations experienced by the peptide at ambient conditions. These data suggest that the 4e motif may not be as effective in attenuating the translocation of the CPP prior to proteolytic cleavage. As the overall probe structure was examined,

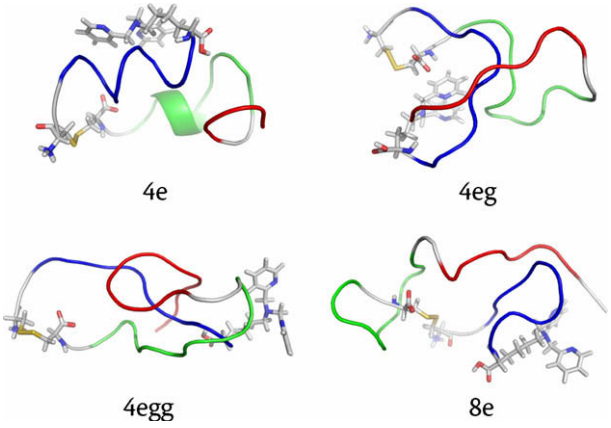

Figure 3. Structures of MMP-14 probes determined from computer simulations using the zipping and assembly method. In each structure, the backbone is shown in a cartoon representation, colored as follows: blue = CCP, green = MMP-14 specific substrate region, and red = attenuating domain. Both the Single Amino Acid Chelate (SAAC) residue and the cysteine–cysteine linker unit are shown in bond representation.

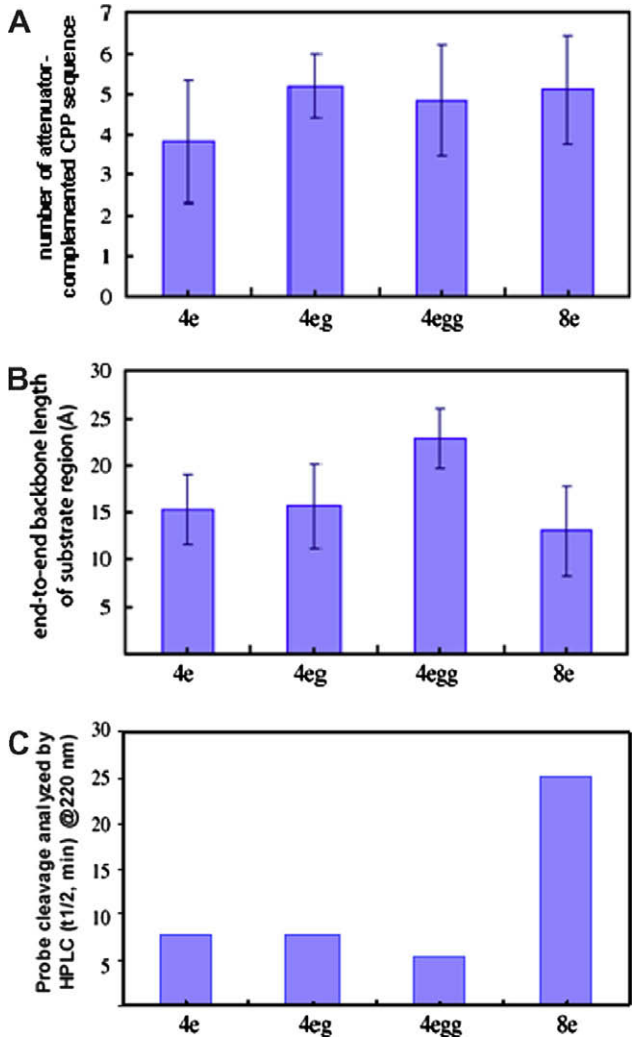

Figure 4. Calculated structural metrics for the four peptides and side-by-side comparison to experimental cleavage data. (A) The computed average (over the structural ensemble) number of arginine residues in the CPP that are in contact with at least one glutamate residue in the attenuating region. (B) The computed average end-to-end distance (Å) of the MMP-14 substrate region; larger values indicate that the substrate is closer to a linear conformation. The error bars show the average fluctuations over the conformational ensemble. (C) Parallel cleavage studies; half-life ($t1/2$, in min) of each probe measured in the presence of MMP-14 by HPLC peak integrations at an absorbance of 220 nm.

the CPP-attenuator complementation was also found to influence the conformation of the MMP-14 substrate region, potentially altering the accessibility for proteolytic cleavage. As the end-to-end distance of the MMP-14 substrate is a direct measure of peptide folding, it also indirectly predicts the availability of the peptide substrate for cleavage. The calculations show (Fig. 4B) that the 4egg probe best adapts the β-strand conformation[33] required for rapid MMP-14 cleavage, exhibiting the longest end-to-end distance of 21.62 ± 4.3 Å. The 4e (16.9 ± 2.9 Å) and 4eg (17.1 ± 4.3 Å) sequences show a similar degree of folding, whereas the 8e probe is the most distorted from linearity (15.0 ± 2.9 Å). This modeling study predicts that the 4egg probe has adequate CPP attenuation in the absence of MMP-14 and allows a β-strand type conformation for the substrate portion of the probe to bind and interact with the MMP-14 catalytic domain.

2.3. Parallel probe synthesis

A modular approach to the panel design was adapted to accelerate the synthesis of the peptide probes. Each probe was retrosynthetically divided into two fragments of comparable size. One peptide fragment common to all of the probes contains the CPP and the SAAC with an additional cysteine and glycine appended to the N-terminus. Four variable fragments, containing the SGRIGF↓LRTA sequence and the attenuators, were also appended with glycine and cysteine at the C-terminus. This allowed all five fragments (1 conserved, 4 specific to each probe) to be synthesized in parallel and to be subsequently assembled into the probe construct (Fig. 2) through simple disulfide chemistry.

Typical synthesis of the various probes yielded the desired constructs along with two homo-dimers. The isolated probes were characterized by analytical HPLC, MALDI-MS and ^{1}H NMR. As expected, the desired MMP-14 probes exhibited retention times between the homo-dimer peaks. MALDI-MS analysis showed the expected molecular ion peak along with the characteristic fragmentation pattern produced by homolytic cleavage of the disulfide bond and loss of pyridylmethylene radicals from the SAAC (Fig. 5).

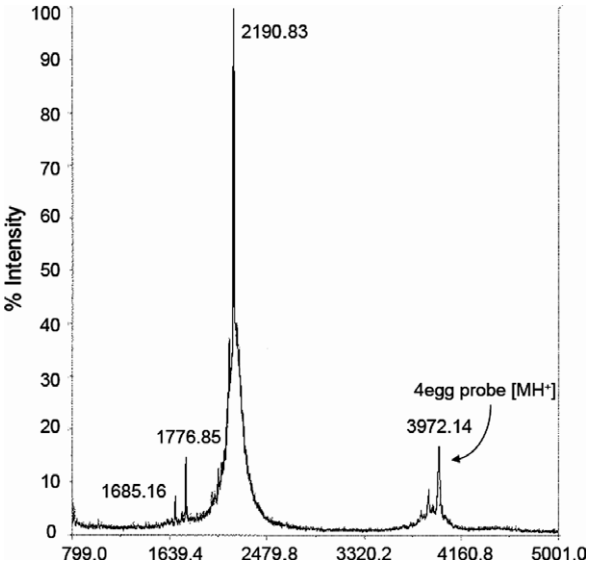

Figure 5. A sample MALDI-MS of the 4egg probe. The presence of the molecular ion peak (3972 amu, $[MH]^{+}$), peptide fragments corresponding to disulfide scission (2191 and 1777 amu), and a fragment corresponding to loss of a pyridylmethylene radical from the SAAC-containing parent peptide (1685 amu = 1777–92).

2.4. Proteolytic cleavage study with purified MMP-14 enzyme

A sample of each probe was subjected to enzymatic digestion by MMP-14, followed by HPLC analysis. As expected, each probe generated two clear cleavage products upon proteolysis, indicating that the cleavage event was largely restricted to a single cleavage site. The cleavage rate was characterized by the probe half-lives and initial cleavage velocities based on the first-order kinetics. Significant differences in cleavage rates between the probes were observed. As shown in Figure 4C, the increasing cleavage rate rank order was 8e < 4e ≈ 4eg < 4egg. Regression analyses confirm that all eight data sets are strongly linear, with r^2 values ranging from 0.90 to 0.99. These data correlate well with the end-to-end distance measures derived from the molecular modeling studies where the 8e probe MMP-14 substrate was most distorted from linearity, the 4e and 4eg probes were similar length yet longer than the 8e probe, while the 4egg probe possessed the longest end-to-end distance.

As previously suggested by Smith and co-workers,[33] the SGRIGF↓LRTA cleavage sequence is believed to possess the β-strand conformation for efficient binding to MMP-14 and to facilitate the subsequent catalytic reaction. In the present study, protein structure related to the interaction of the attenuator with the CPP changes the embedded MMP-14 substrate conformation directly affecting the cleavage rate. The molecular modeling of this small library of structures efficiently predicts the cleavage rate as a function of substrate linearity. Thus, the attenuation sequence may be chosen for effective attenuation of the CPP and presentation of an optimized structural conformation for rapid enzymatic cleavage.

2.5. Radiochemistry with ^{99m}Tc

The carboxylate terminal of the r_8 CPP was linked to a single amino acid chelate (SAAC) through a peptide bond. Based on our results in molecular modeling and MMP-14 cleavage study, the optimal probe, 4egg, was chosen to demonstrate labeling efficiency. The 4egg probe was successfully labeled with technetium-99m through the $[^{99m}Tc(CO)_3(OH_2)_3]^{+}$ intermediate. The final ^{99m}Tc- labeled probe was isolated by HPLC with 97% radiopurity and a radiochemical yield greater than 90%.

The SAAC technology, developed by Zubieta and colleagues, has shown great promise in small molecule radiopharmaceutical applications.[35,37,38] The SAAC, a lysine based residue with a built-in chelating system for binding rhenium or technetium tricarbonyl, was chosen over direct peptide labeling techniques to avoid non-specific binding of the label on the backbone structure. The SAAC also allows labeling of the molecule as the final step. Labeling an intermediate that is subsequently reacted with the final molecule may reduce yield, while bulky chelating molecules or bifunctional chelates used in direct labeling may significantly effect biodistribution of the labeled compound.[39] For instance, Polyakov and colleagues have synthesized a Tat CPP incorporating a peptide-based motif (epsilon-KGC) that provides an N_3S donor core for chelating technetium and rhenium. They have successfully demonstrated its uptake in Jurkat cells after labeling with oxotechnetium(V) or oxorhenium(V).[40] Although this approach offers labeling specificity, each donor core requires three additional residues. The current probe design and prototype, on the other hand, utilizes a single residue for each technetium or rhenium tag. In addition, this strategy for radiolabeling provides control over the isotope delivery system thereby permitting the MMP-14 probe to be labeled with technetium-99m (a pure gamma emitter) or rhenium-186 (a beta and gamma emitter) that will not only allow early detection of invasive cancer, but it will also provide a common platform for radiotherapy.

2.6. In vitro uptake of the ^{99m}Tc labeled probe

Human epithelial breast cancer (MDA-MB-231) cells transfected with MMP-14 cDNA to overexpress MMP-14[41] were used to evaluate the in vitro uptake of the labeled 4egg probe. The effect of probe activation through cleavage by MMP-14 at cell surface was determined by treatment of the transfected MDA-MB-231 cells with and without the potent broad-based MMP inhibitor, GM1489. Free ^{99m}Tc-tricarbonyl complex was compared as a null control. All cell studies were carried out in triplicate. After the treatment with the labeled 4egg probe, the adhesive cells were carefully washed with DMEM, before being released from the plate with trypsin. The probe content within each media and cell fraction was then quantified by a gamma counter (Wizard 3, Perkin–Elmer, CT). Each data point represents the fraction of the probe uptake by cells quantified by gamma count before and after incubation and washings of cells (approximately 10^5 cells per well). As shown in Figure 6, there is a clear difference in the cellular uptake of probe in the presence and absence of the MMP inhibitor. There was little or no uptake of the free $[Tc(CO)_3]^+$ by the cells. Despite the larger variation in cells without inhibitor (may due to cell handling), the average uptake of the 4egg probe was two times greater in cells without inhibitor compared to those with inhibitor. This demonstrates the successful cleavage and increased uptake of the activated probe into MMP-14 expressing cells. The residual 10–15% uptake in cells treated with MMP inhibitor indicates that there may be incomplete inhibition of MMP-14 activity by the inhibitor, or a basal level of probe leakage attributable to incomplete attenuation of the CPP. The negative results from $[^{99m}Tc(CO)_3]^+$ suggests that (a) there is no non-specific uptake of free $[^{99m}Tc(CO)_3]^+$ and (b) the positive uptake of the probe is the result of the cleaved probe rather than leakage of free $[^{99m}Tc(CO)_3]^+$ into the transfected cells. Attempts have been made to use MDA-MB-231 cells without MMP-14 transfection as a negative control. However, uptake of the 4egg probe was also observed. This may due to cleavage reactions by combination of other MMPs at basal level.[33] Nevertheless, the reduction in uptake by transfected cells in the presence of inhibitor suggests that the 4egg probe possesses MMP-14 specificity, and it warrants further efforts in probe development.

3. Conclusion

The unique application of molecular modeling in optimization of the MMP-14 probe construct has been demonstrated. Modeling calculations were able to provide useful information on the attenuation properties of four different sequences against the r_8 CPP and the length of the MMP substrate that is directly related to cleavage rate. Both of attenuation and cleavage must be maximized in the optimal probe. Although three out of four probes studied exhibited good CPP attenuation, the CPP/attenuator interaction contributed to structural modifications of the MMP-14 substrate altering the cleavage rate. The probe with the longest end-to-end substrate length, 4egg, exhibited the fastest cleavage rate. Evaluation of the 4egg probe in cells expressing MMP-14 demonstrated the specific activation of the probe and subsequent accumulation of the label in the cell. The value of computational modeling to imaging probe design has been demonstrated and this methodology will be incorporated into future tumor imaging probe platform development.

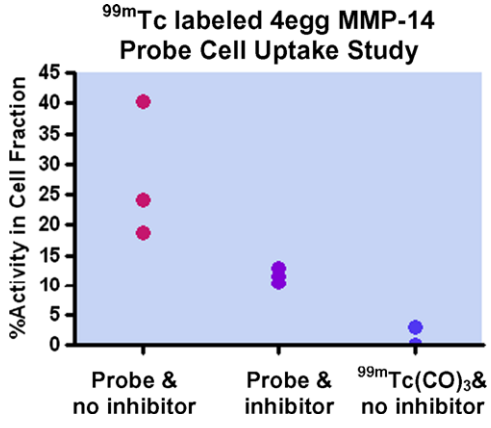

Figure 6. In vitro uptake of the 4egg probe in MMP-14 expressing MDA-MB-231 cells with and without metalloproteinase inhibitor. $[Tc(CO)_3]^+$ was used as a negative control.

4. Experimental

4.1. Molecular modeling

Computer simulations were used to predict the solution structures of the peptide probes employing the AMBER96 force field[42] with the implicit solvation model of Onufriev, Bashford, and Case.[43] This force field was validated in a separate study and shown to give accurate structures for peptides with both alpha and beta motifs.[44] For the non-canonical chelate residue, the program 'antechamber' in the AMBER package was used to determine atomic charges and estimate force field constants. The SAAC chelate was included in the molecule without the radiometal for the simulations.

Sampling was performed using the zipping and assembly (Z&A) methodology developed by the Dill research group.[45] Z&A works by sampling peptides and proteins according to a putative folding mechanism:[46] peptide pieces along the chain independently first form small bits of structure, which then either nucleate additional structure locally by reeling in nearby sections of chain (zipping), or join together with other such structured peptide pieces to form larger units (assembly). This mechanism is implemented in simulation by first breaking a peptide into small fragments, which are simulated separately, and then by growing these fragments by the addition of new residues and other fragments, followed in each case by further simulation. Sampling at each stage is performed using replica exchange molecular dynamics.[47]

For each of the probe candidates, the overall chain was broken into the three fragments corresponding to the attenuator, substrate, and translocation domains. These were simulated separately in replica exchange for 10 ns, and conformations from each fragment from the final 1 ns were clustered into a maximum of 10 structures using a modified k-means algorithm. Subsequently, clustered conformations from the substrate and translocation domains were combined (in all permutations), and used in a second 10 ns replica exchange simulation, followed by additional clustering. Next, the attenuating domain structures were added, followed by 10 ns of sampling, and finally, the terminal chelate residue was added, with 30 ns of replica exchange as the last sampling step. The clustered conformations from the last 5 ns of the 30 ns run (along with their populations) were taken as the final conformational ensemble. In total, each peptide required about 300 aggregate CPU days worth of simulation time on Xeon 2.4 GHz processors.

4.2. MMP-14 probe synthesis

Uronium coupling agents (2-(1*H*-9-azabenzotriazole-1-yl)-1,1,3,3-tetramethyluronium hexafluorophosphate or tetrafluoroborate; 'HATU' and 'TBTU') and Fmoc-protected amino acids were purchased from Novabiochem, Inc. The Nα-Fmoc-Nε-bis(pyridylmethyl)-lysine was received from Molecular Insight Pharmaceuticals, Inc. or synthesized as previously described.[42] Solvents, including dichloromethane and dimethylformamide, were pur-

chased from VWR Scientific. All other reagents were obtained from Sigma–Aldrich Chemical Company, and used without further purification.

Peptide intermediates were synthesized on a Protein Technologies, Inc. Prelude peptide synthesizer according to standard Fmoc chemistry protocols. In some cases, Fmoc deproptections were effected using 6% piperazine in dimethylformamide,[48] as opposed to the more traditional 20% piperidine in DMF. All sequences were cleaved from the resin and deprotected using 92:3:3:1:1 trifluoroacetic acid/triisoproylsilane/water/thioanisole/1-naphthol for 2 h. Crude peptides were obtained by triturating the cleavage solution with ice-cold ether, followed by centrifugation. All peptide starting materials were purified by semi-preparative, reverse-phase HPLC (Jupiter C12 column from Phenomenex; water-acetonitrile gradient, 95% water to 5% water; 0.1% trifluoroacetic acid added to the mobile phase to maintain a pH ~2.)

The completed probes were assembled as heterodimeric disulfides. Cysteine oxidation was conducted using the following general procedure: Ac-CGrrrrrrrrr(SAAC)-$CONH_2$ (~1.8 mg.; 1 μmol) and a suitable attenuator-MMP-14 substrate peptide (~3 to 4 mg., according to the mass of the attenuator sequence; 1 μmol) were dissolved in 0.75 mL of 5:3:2 water/0.2 M borate buffer, pH 8/methanol. The peptides were pre-reduced by addition of 50 μL of 1 mg/mL tris-(2-carboxyethyl)phosphine hydrochloride, dissolved in the same reaction buffer. After 15 min, the pH was checked to ensure the reaction mixture remained above 8; then, 100 μL of DMSO was added with swirling, followed 5 min later by 5 mg. of potassium hexacyanoferrate (III). The resulting yellow solution was covered with foil, and allowed to stand overnight. Following acidification with 50 μL of acetic acid, the reaction mixture was diluted to ca. 1 mL with deionized water, and purified by semi-preparative HPLC (Jupiter C12 column from Phenomenex; water–acetonitrile gradient, 95% water to 5% water; 0.1% trifluoroacetic acid added to the mobile phase to maintain a pH ~2.) Typically, three major peaks were observed at 220 nm (two peaks at 260 nm), corresponding to the desired heterodimer and homodimerized reactants. The reactant homodimers could be recovered and reductively recycled for use in future reactions.

4.3. MMP-14 cleavage kinetics

Approximately equimolar samples of each unlabeled probe were prepared in MMP-14 hydrolysis buffer (50 mM Tris–HCl, pH 7.5, 150 mM NaCl, 5 mM $CaCl_2$, 0.025% Brij-35)[49] as verified by HPLC analysis and peak integration at 260 nm. Each of these peptide stock solutions (0.8 mL) was transferred to a separate microcentrifuge tube, and equilibrated at 37 °C for 30 min. Recombinant MMP-14 catalytic domain was obtained from Calbiochem, at a concentration of 200 μg/mL. This solution was diluted by half with assay buffer, and 4 μL of the resulting solution was transferred to each probe solution. Aliquots of each solution (25 μL) were removed at time points of 0, 2.5, 5, 7.5, 10, 20, 40, 80, and 120 min, and rapidly transferred to an HPLC vial insert containing 50 μL of ice-cold quenching reagent (0.1 M EDTA/2 Na^+ in 1% HOAc, pH 3). The quenched samples were then analyzed by RP-HPLC (Jupiter C12 analytical column (Phenomenex), flow rate 1.1 mL/min 0–5 min, 95% water, 5% acetonitrile, 0.1% TFA; 5–35 min, ramp to 50% water, 50% acetonitrile, 0.1% TFA; then, re-equilibration at 95% water).

Probe half-lives and initial cleavage velocities were extracted from the analytical HPLC data, assuming enzyme saturation and first-order probe cleavage kinetics early in the reaction time course. For the 4e, 4eg, and 4egg probes, linear curves were constructed by plotting the natural log of the intact probe peak area against time. For these probes, saturation conditions were assumed to persist until the 20 min time point. The 8e probe data was analyzed in a similar fashion, and included the 40 min time point in the analysis. Calculations were conducted twice for each probe, using HPLC data obtained at either 220 or 260 nm. The slope of each linear equation was taken as a measure of initial cleavage velocity. Probe half-lives were estimated by dividing the measured probe peak areas at $t = 0$ in half, and substituting the resulting values into each regression equation to solve for t.

4.4. ^{99m}Tc radiochemistry

Radiolabeling of the probes with ^{99m}Tc was carried out using an IsoLink tricarbonyl labeling kit (Covidien Inc., MO), via a modified procedure. Briefly, a solution of $[^{99m}TcO_4]^-$ (1 mL) from a commercial generator (20–100 mCi) was added to a sealed vial containing sodium boranocarbonate (4.5 mg), sodium tetraborate dodecahydrate (2.85 mg), sodium tartrate dehydrate (8.5 mg) and sodium carbonate (7.15 mg). The reaction mixture was warmed in a boiling water bath for 20 min to form an intermediate complex of $[^{99m}Tc(CO)_3(OH_2)_3]^+$. The pH was adjusted to 6–6.5 using 1 M HCl. This stock solution (200 μL) was then reacted with the unlabeled probe (25–50 nmol dissolved in 100 μL of methanol) at 75 °C for 15–30 min. The final ^{99m}Tc- labeled probe was isolated by HPLC at high purity (90% radiological yield).

4.5. In vitro cell studies

Human epithelial breast cancer (MDA-MB-231) cells transfected with MMP-14 cDNA to overexpress MMP-14 were cultured and characterized using published methods.[41] They were distributed into six-well plates (100,000 cells per well). The plates were incubated overnight. The MMP-14 inhibitor buffer was prepared by dissolving EDTA-disodium salt and GM 1469 metalloprotease inhibitor in DMEM media, to concentrations of 1.0 mM and 0.2 mM, respectively. Aliquots of inhibitor solution (100 μL) were added to three of the wells; the remaining wells received 100 μL aliquots of blank DMEM media. All wells were then incubated for 20 min. Six wells (three treated with inhibitor, three untreated) were spiked with 33 μL (16.5 μL) of ^{99m}Tc radiolabeled probe in PBS. The remaining three wells received 33 μL (16.5 μL) of free ^{99m}Tc tricarbonyl complex in PBS as a negative control. Following 20 min. of incubation time, the medium was removed from each plate, and adhesive cells were washed with an additional 1 mL of DMEM. All media washes were collected in separate microcentrifuge tubes. The adhesive cells were then collected by washing each plate three times with trypsin solution (1 mL per plate; 2 × 2 min, 1 × 30 min), and once with methanol (1 mL per plate; 2 min). Each wash was again collected in a separate microcentrifuge tube. The ^{99m}Tc content of every collected fraction was then quantified by gamma counter.

Acknowledgements

This work was supported by the Office of Science, Office of Biological and Environmental Research, Biological Systems Science Division, U.S. Department of Energy (DE-FG02-05ER64010). G.W. was supported by a Department of Defense Breast Cancer Center of Excellence grant DAMD17-02-1-0693, and L.M.C. acknowledges R01 support from the NIH/NCI and a DOD BCRP Era of Hope Scholar Award (W81XWH-06-1-0416).The authors wish to thank Molecular Insight Pharmaceuticals, Inc. for their gift of the dipyridyl-lysine SAAC.

References and notes

1. Seiki, M. *Cancer Lett.* **2003**, *194*, 1–11.
2. Sternlicht, M. D.; Bissell, M. J.; Werb, Z. *Oncogene* **2000**, *19*, 1102–1113.

3. Cai, W.; Rao, J.; Gambhir, S. S.; Chen, X. *Mol. Cancer Ther.* **2006**, *5*, 2624–2633.
4. Overall, C. M.; Lopez-Otin, C. *Nat. Rev. Cancer* **2002**, *2*, 657–672.
5. Scherer, R. L.; McIntyre, J. O.; Matrisian, L. M. *Cancer Metastasis Rev.* **2008**, *27*, 679–690.
6. Van de Wiele, C.; Oltenfreiter, R. *Cancer Biother. Radiopharm.* **2006**, *21*, 409–417.
7. Zucker, S.; Cao, J. *Nat. Med.* **2001**, *7*, 655–656.
8. Page-McCaw, A.; Ewald, A. J.; Werb, Z. *Nat. Rev. Mol. Cell Biol.* **2007**, *8*, 221–233.
9. Zucker, S.; Pei, D.; Cao, J.; Lopez-Otin, C. *Curr. Top. Dev. Biol.* **2003**, *54*, 1–74.
10. Sounni, N. E.; Noel, A. *Biochimie* **2005**, *87*, 329–342.
11. Strongin, A. Y.; Collier, I.; Bannikov, G.; Marmer, B. L.; Grant, G. A.; Goldberg, G. I. *J. Biol. Chem.* **1995**, *270*, 5331–5338.
12. Sakakibara, M.; Koizumi, S.; Saikawa, Y.; Wada, H.; Ichihara, T.; Sato, H.; Horita, S.; Mugishima, H.; Kaneko, Y.; Koike, K. *Cancer* **1999**, *85*, 231–239.
13. Michael, M.; Babic, B.; Khokha, R.; Tsao, M.; Ho, J.; Pintilie, M.; Leco, K.; Chamberlain, D.; Shepherd, F. A. *J. Clin. Oncol.* **1999**, *17*, 1802.
14. Yoshizaki, T.; Maruyama, Y.; Sato, H.; Furukawa, M. *Int. J. Cancer* **2001**, *95*, 44–50.
15. Yoshizaki, T.; Sato, H.; Maruyama, Y.; Murono, S.; Furukawa, M.; Park, C. S.; Seiki, M. *Cancer* **1997**, *79*, 139–144.
16. Kanayama, H.; Yokota, K.; Kurokawa, Y.; Murakami, Y.; Nishitani, M.; Kagawa, S. *Cancer* **1998**, *82*, 1359–1366.
17. Davidson, B.; Goldberg, I.; Gotlieb, W. H.; Kopolovic, J.; Ben-Baruch, G.; Nesland, J. M.; Reich, R. *Mol. Cell Endocrinol.* **2002**, *187*, 39–45.
18. Bremer, C.; Bredow, S.; Mahmood, U.; Weissleder, R.; Tung, C. H. *Radiology* **2001**, *221*, 523–529.
19. Bremer, C.; Tung, C. H.; Weissleder, R. *Nat. Med.* **2001**, *7*, 743–748.
20. Chen, J.; Tung, C. H.; Allport, J. R.; Chen, S.; Weissleder, R.; Huang, P. L. *Circulation* **2005**, *111*, 1800–1805.
21. Jiang, T.; Olson, E. S.; Nguyen, Q. T.; Roy, M.; Jennings, P. A.; Tsien, R. Y. *Proc. Natl. Acad. Sci. U.S.A.* **2004**, *101*, 17867–17872.
22. McIntyre, J. O.; Fingleton, B.; Wells, K. S.; Piston, D. W.; Lynch, C. C.; Gautam, S.; Matrisian, L. M. *Biochem. J.* **2004**, *377*, 617–628.
23. Zhang, Y.; So, M. K.; Rao, J. *Nano Lett.* **2006**, *6*, 1988–1992.
24. Breyholz, H. J.; Schafers, M.; Wagner, S.; Holtke, C.; Faust, A.; Rabeneck, H.; Levkau, B.; Schober, O.; Kopka, K. *J. Med. Chem.* **2005**, *48*, 3400–3409.
25. Furumoto, S.; Takashima, K.; Kubota, K.; Ido, T.; Iwata, R.; Fukuda, H. *Nucl. Med. Biol.* **2003**, *30*, 119–125.
26. Giersing, B. K.; Rae, M. T.; CarballidoBrea, M.; Williamson, R. A.; Blower, P. J. *Bioconjugate Chem.* **2001**, *12*, 964–971.
27. Kopka, K.; Breyholz, H. J.; Wagner, S.; Law, M. P.; Riemann, B.; Schroer, S.; Trub, M.; Guilbert, B.; Levkau, B.; Schober, O.; Schafers, M. *Nucl. Med. Biol.* **2004**, *31*, 257–267.
28. Medina, O. P.; Kairemo, K.; Valtanen, H.; Kangasniemi, A.; Kaukinen, S.; Ahonen, I.; Permi, P.; Annila, A.; Sneck, M.; Holopainen, J. M.; Karonen, S. L.; Kinnunen, P. K.; Koivunen, E. *Anticancer Res.* **2005**, *25*, 33–42.
29. Oltenfreiter, R.; Staelens, L.; Lejeune, A.; Dumont, F.; Frankenne, F.; Foidart, J. M.; Slegers, G. *Nucl. Med. Biol.* **2004**, *31*, 459–468.
30. Sprague, J. E.; Li, W. P.; Liang, K.; Achilefu, S.; Anderson, C. J. *Nucl. Med. Biol.* **2006**, *33*, 227–237.
31. Zheng, Q. H.; Stone, K. L.; Mock, B. H.; Miller, K. D.; Fei, X.; Liu, X.; Wang, J. Q.; Glick-Wilson, B. E.; Sledge, G. W.; Hutchins, G. D. *Nucl. Med. Biol.* **2002**, *29*, 803–807.
32. Goun, E. A.; Shinde, R.; Dehnert, K. W.; Adams-Bond, A.; Wender, P. A.; Contag, C. H.; Franc, B. L. *Bioconjugate Chem.* **2006**, *17*, 787–796.
33. Kridel, S. J.; Sawai, H.; Ratnikov, B. I.; Chen, E. I.; Li, W.; Godzik, A.; Strongin, A. Y.; Smith, J. W. *J. Biol. Chem.* **2002**, *277*, 23788–23793.
34. Wender, P. A.; Mitchell, D. J.; Pattabiraman, K.; Pelkey, E. T.; Steinman, L.; Rothbard, J. B. *Proc. Natl. Acad. Sci. U.S.A.* **2000**, *97*, 13003–13008.
35. Stephenson, K. A.; Zubieta, J.; Banerjee, S. R.; Levadala, M. K.; Taggart, L.; Ryan, L.; McFarlane, N.; Boreham, D. R.; Maresca, K. P.; Babich, J. W.; Valliant, J. F. *Bioconjugate Chem.* **2004**, *15*, 128–136.
36. Levadala, M. K.; Banerjee, S. R.; Maresca, K. P.; Babich, J. W.; Zubieta, J. *Synthesis* **2004**, 1759–1766.
37. Banerjee, S. R.; Levadala, M. K.; Lazarova, N.; Wei, L.; Valliant, J. F.; Stephenson, K. A.; Babich, J. W.; Maresca, K. P.; Zubieta, J. *Inorg. Chem.* **2002**, *41*, 6417–6425.
38. Banerjee, S. R.; Wei, L.; Levadala, M. K.; Lazarova, N.; Golub, V. O.; O'Connor, C. J.; Stephenson, K. A.; Valliant, J. F.; Babich, J. W.; Zubieta, J. *Inorg. Chem.* **2002**, *41*, 5795–5802.
39. Bullok, K. E.; Dyszlewski, M.; Prior, J. L.; Pica, C. M.; Sharma, V.; Piwnica-Worms, D. *Bioconjugate Chem.* **2002**, *13*, 1226–1237.
40. Polyakov, V.; Sharma, V.; Dahlheimer, J. L.; Pica, C. M.; Luker, G. D.; Piwnica-Worms, D. *Bioconjugate Chem.* **2000**, *11*, 762–771.
41. Tam, E. M.; Morrison, C. J.; Wu, Y. I.; Stack, M. S.; Overall, C. M. *Proc. Natl. Acad. Sci. U.S.A.* **2004**, *101*, 6917–6922.
42. Cornell, W. D.; Cieplak, P.; Bayly, C. I.; Gould, I. R.; Merz, K. M.; Ferguson, D. M.; Spellmeyer, D. C.; Fox, T.; Caldwell, J. W.; Kollman, P. A. *J. Am. Chem. Soc.* **1995**, *117*, 5179–5197.
43. Onufriev, A.; Bashford, D.; Case, D. A. *Proteins* **2004**, *55*, 383–394.
44. Shell, M. S.; Ritterson, R.; Dill, K. A. *J. Phys. Chem. B* **2008**, *112*, 6878.
45. Ozkan, S. B.; Wu, G. A.; Chodera, J. D.; Dill, K. A. *Proc. Natl. Acad. Sci. U.S.A.* **2007**, *104*, 11987–11992.
46. Fiebig, K. M.; Dill, K. A. *J. Chem. Phys.* **1993**, *98*, 3475–3487.
47. Sugita, Y.; Okamoto, Y. *Chem. Phys. Lett.* **1999**, *314*, 141–151.
48. Wade, J. D.; Mathieu, M. N.; Macris, M.; Tregear, G. W. *Lett. Peptide Sci.* **2000**, *7*, 107–112.
49. Gupta, P. D.; Waheed, A. A. *FEBS Lett.* **1992**, *300*, 263–267.